Phase Transition in the Near-Surface Region of Ternary Pb(In_{1/2}Nb_{1/2})O_{3}-Pb(Mg_{1/3}Nb_{2/3})O_{3}-PbTiO_{3} Relaxor Ferroelectric Crystals

Yaojin Wang, Guoliang Yuan, Haosu Luo, Jiefang Li, and D. Viehland

Phys. Rev. Applied **8**, 034032 — Published 27 September 2017

DOI: 10.1103/PhysRevApplied.8.034032

Phase transition in the near-surface region of ternary $Pb(In_{1/2}Nb_{1/2})O_3$-$Pb(Mg_{1/3}Nb_{2/3})O_3$-$PbTiO_3$ relaxor ferroelectric crystals

Yaojin Wang[1, 2, a)], Guoliang Yuan[1], Haosu Luo[3], Jiefang Li[4], D. Viehland[4]

[1] *School of Materials Science and Engineering, Nanjing University of Science and Technology, Nanjing 210094, Jiangsu, China*

[2] *MIIT Key Laboratory of Advanced Display Materials & Devices, Nanjing 210094, Jiangsu, China*

[3] *Shanghai Institute of Ceramics, Chinese Academy of Sciences, 215 Chengbei Road, Jiading, Shanghai 201800, China*

[4] *Materials Science and Engineering, Virginia Tech, Blacksburg, Virginia 24061, USA*

Relaxor ferroelectric single crystals have been documented to possess a skin effect in the near-surface region, which may play an important role in emerging micro-/nano-scale piezoelectric devices that are surface-dominated. Here, a metastable ferroelectric tetragonal phase is induced by an electric field applied above the Curie temperature (i.e., poling at high temperature) in rhombohedral structured $Pb(In_{1/2}Nb_{1/2})O_3$-$Pb(Mg_{1/3}Nb_{2/3})O_3$-$PbTiO_3$ ternary relaxor ferroelectric crystals. Most interestingly, this metastable tetragonal structure unexpectedly transforms into a monoclinic *B*-type (M_B) phase, as revealed by reciprocal-space mesh scans via high-resolution x-ray diffraction. The domain configurations of the M_B phase obtained by poling above the Curie temperature are similar to that obtained by poling at room

temperature; however, the bulk piezoelectricity is extremely weak relative to that induced by the latter process. This controversy between microstructure and macro-property is understood by a "surface-interior" heterogeneous structure, which sheds insight into the existence of skin effects in the relaxor ferroelectric single crystals.

[a] Electronic mail: yjwang@njust.edu.cn

I. INTRODUCTION

Relaxor ferroelectric solid solutions have attracted much attention in materials science and applied/condensed matter physics communities due to their unprecedented piezoelectric response and fascinating underlying mechanisms[1-3]. These materials, such as binary $Pb(Mg_{1/3}Nb_{2/3})O_3$-$PbTiO_3$ (PMN-PT), $Pb(Zn_{1/3}Nb_{2/3})O_3$-$PbTiO_3$ (PZN-PT), and ternary $Pb(In_{1/2}Nb_{1/2})O_3$-$Pb(Mg_{1/3}Nb_{2/3})O_3$-$PbTiO_3$ (PIN-PMN-PT) crystals, are finding applications in sensors[4], actuators[5], and medical ultrasonics[1], which show great potential to displace the market-dominating lead zirconate (PZT) ceramic system[1,2]. In particular, with regards to efforts towards device miniaturization, epitaxial thin films of these emerging alternative materials with superior piezoelectricity have also been achieved in next-generation hyperactive micro/nano-electromechanical systems (MEMS/NEMS) for acoustic sensors and mechanical energy harvesting devices[6,7]. Their extraordinarily high piezoelectricity in both bulk crystals and micro-/nano-meter films has been generally attributed to the presence of a vertical

morphotropic phase boundary (MPB) in the temperature-composition phase diagram[8,9], which bridges rhombohedral (*R*) and tetragonal (*T*) phases[10,11]. In the vicinity of the MPB, three different types of low-symmetry monoclinic phases (i.e., M_A, M_B and M_C) have been experimentally found and theoretically predicted[10,12-14]. Such fascinating phase behavior around the MPB provides structural information on which to clarify the origin of the ultrahigh piezoelectricity in these materials, as the polarization vectors of the monoclinic phases are unconstrained within a plane, rather than being confined to a particular crystallographic axis as those of higher symmetry *R* or *T* phases[15]. It is still unclear whether these monoclinc symmetries are intrinsic homogeneous phases, or rather a higher-symmetry structually-adaptive heterogeonous one[16-19]. Either way, these low symmetries produce an easy polarization rotation pathway relative to the high-symmetry phases, which in turn results in enhanced piezoelectricity[9,19,20].

Another interesting feature of relaxor ferroelectric single crystals is that they can exhibit skin effects[21,22], where crystals have a depth-dependent lattice parameter(s) and symmetry on a scale of several micrometers[23-25]. We parenthetically note that such skin effect has also been reported in non-relaxor $SrTiO_3$[26]. Controversy remains concerning whether this skin effect stems from an intrinsic symmetry difference between the near-surface region and bulk, or rather from extrinsic mechanical polishing-induced symmetry-breaking of the surface[24]. The skin effect is further complicated in these materials due to their proximity to the MPB, which will further broaden the diffraction peaks and produce diffraction profiles that are dependent on

incident beam energy[21]. In view of the scale of the piezoelectric materials in MEMS/NEMS sensors and energy conversion devices, such a skin effect would play an important role in device performance (such as thermal stability, electromechanical response efficiency) as the volume fraction of the surface layer is significant in these MEMS/NEMS devices. In the past, most investigations that involved skin effects focused on different microstructures between near-surface and interior volumes of crystals[3,21,24], disregarding differences between the micro-structure of the near-surface layer and the properties of the bulk.

In this paper, we demonstrate an inconsistent relationship between the micro-structure in the near-surface region and the piezoelectricity of the bulk, shedding light on the skin effect of relaxor ferroelectric single crystals. An electric field induced metastable ferroelectric tetragonal phase was found above the Curie temperature in ternary PIN-PMN-PT crystals by high-resolution x-ray diffraction. This metastable *T* phase unexpectedly transformed into a M_B one after zero-field-cooling to room temperature, rather than to a signature high-symmetry *R* phase as expected from a traditional annealing process. More interestingly, crystals of this M_B phase exhibit a much smaller bulk piezoelectric constant d_{33}, relative to the M_B phase obtained after conventional poling at room temperature. These findings present a framework for elucidating the essential physics of the unique piezoelectricity in the surface-dominated emerging micro-/nano-scale piezoelectric devices.

II. EXPERIMENTAL DETAILS

Ternary relaxor ferroelectric single crystals with a nominal composition of 33PIN-35-PMN-32PT were grown from the melt by a modified Bridgman method. The as-grown crystals were oriented along the pseudocubic [110]/[1-10]/[001] crystallographic axes using x-ray diffraction, and then diced into cube-shaped samples with dimensions of $2\times2\times2$ mm^3 from the rhombohedral region of the crystal boule[15,27,28]. The $(110)_{PC}$ and $(001)_{PC}$ faces of the specimens were polished to a smoothness of 0.25μm. The cube specimens were used for dielectric measurements and XRD characterization, after depositing gold electrodes on the $(110)_{PC}$ faces of the cubes. For comparison, non-relaxor ferroelectric single crystals of $BaTiO_3$ with dimensions of $2\times2\times0.5$ mm^3 were prepared with their thickness direction parallel to $[110]_{PC}$, and were polished to a smoothness of 0.25 μm. All specimens were annealed at 800K for 30 min to release the residual stress introduced by crystal growth and mechanical polishing.

The temperature dependence of the dielectric properties was measured using a Hewlett-Packard 4284A inductance-capacitance-resistance meter equipped with a special tube furnace. The piezoelectric d_{33} constant of the specimens was directly measured using a quasi-static piezoelectric constant meter (ZJ-3A, Institute of Acoustics, Chinese Academy of Science). X-ray diffraction was performed using a Philips MPD high-resolution system equipped with a two-bounce hybrid momochromator, an open three-circle Eulerian cradle, and a domed hot stage. More details about this facility can be found in previous reports[15,23]. The X-ray generator

was operated at 45 kV and 40 mA, and the X-ray penetration depth due to absorption in these Pb-based relaxor ferroelectric crystals was about 1~2 micrometers[23]. Line scans were measured around the $(200)_{PC}$ and $(220)_{PC}$ Bragg peaks under various electrical fields parallel to the $[110]_{PC}$ direction. Electric fields were applied by a high voltage power supply (Bertan, model 205B-10R) via attaching thin wires on the electroded sides using a small drop of conducting epoxy. To better determine the structure, reciprocal-space mesh scans (RMS) were taken around the $(200)_{PC}$ Bragg peaks in the (H0L) zones, and around the $(002)_{PC}$ in the (HHL) zone. The RMS data were obtained by performing a sequence of 2θ-ω scans at different ω offsets, and are shown as intensity as a function of reciprocal lattice position (in rlu)[23].

III. RESULTS AND DISCUSSION

First, the phase transition and ground state of the specimens was characterized by temperature-dependent dielectric constant and high-resolution X-ray diffraction in the zero-field-cooling condition. Figure 1(a) shows the dielectric properties of a [110]-oriented PIN-PMN-PT crystal as a function of temperature at various frequencies. The data clearly shows a broad frequency dispersive maximum over a wide temperature range. This reveals that the ternary PIN-PMN-PT crystal is a typical relaxor ferroelectric, similar to other rhombohedral binary single crystals[29]. It was also found that the dielectric peak around T_m was not associated with a paraelectric to ferroelectric phase transition, as there were no measurable structural variations and diffraction intensity changes. The other two dielectric anomalies around 440K and

355K are consistent with abrupt diffraction angle shifts and intensity changes, as shown in Figure 1 (b). These data indicate a cubic (C)→T →R phase transformation sequence. It is worth noting that the full width of half maximum (FWHM) of the $(002)_C$ peak of relaxor PIN-PMN-PT increased on zero-field-cooling in the cubic phase region, while that for non-relaxor $BaTiO_3$ crystals exhibited a near flat response to temperature variations, as shown in Figure 1(c). Similar changes in FWHM have also observed in binary PMN-PT and PZN-PT relaxor crystals[23]. A likely explanation for this broaden feature is a skin effect in relaxor crystals[21,24], as a low-energy X-ray beam was used in our studies. Figure 1(d) presents representative diffraction peak profiles at various temperatures from 520 K to 300 K, which validate the phase transformation sequence of C→T→R. The data were well fit using single-, double-, and triple-peak Gaussian functions. A cubic structure is evidenced by a strong singlet profile about the $(002)_{PC}$. On cooling to 435 K, the $(002)_{PC}$ diffraction peak split. The profile was fit with a double Gaussian-peak to check whether a high-angle shoulder was the result of a coexisting low volume fraction of tetragonal *a*-domains in the *C* phase matrix. This possibility was verified by a triplet Gaussian-peak fitting on further cooling to 430 K. The high-angle shoulder grew in intensity evidencing a stronger tetragonal *a*-domain state, the high intensity cubic peak was significantly weakened, and a weak shoulder appeared due to a small volume fraction of a tetragonal *c*-domain state. The *T* phase, with coexisting strong *a*-domain and weak *c*-domain peaks, was continuously observed on cooling until a transition into a new structure occurred near 360 K, as shown in Figure 1(d). A single broad peak became

evident along the $(002)_{PC}$ zone, and a (220)-(-220) doublet was observed in the pseudocubic (220) zone (data not shown). The evolution of the line profile reveals a $T \rightarrow R$ transition near 360 K, which agreed well with a dielectric anomaly.

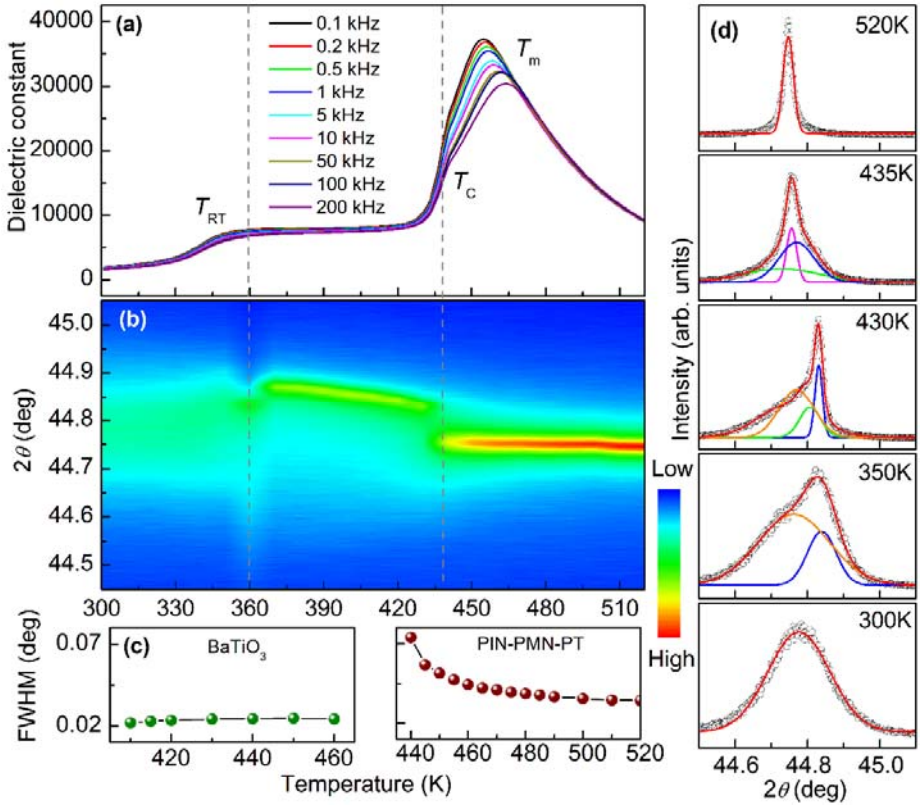

Figure 1 (a) Dielectric constant dependence on temperature under zero-field-cooling condition. (b) Intensity contour map of $(002)_{PC}$ Bragg peaks that show the evolution of phase transformation with temperature under a zero-field-cooling condition. (c) Full width of half maximum (FWHM) of the $(002)_{PC}$ Bragg peak of non-relaxor ferroelectric $BaTiO_3$ and relaxor ferroelectric PIN-PMN-PT single crystals in the cubic phase region. (d) Diffraction peaks along the $(002)_{PC}$ at various temperatures for PIN-PMN-PT crystals under zero-field-cooling condition.

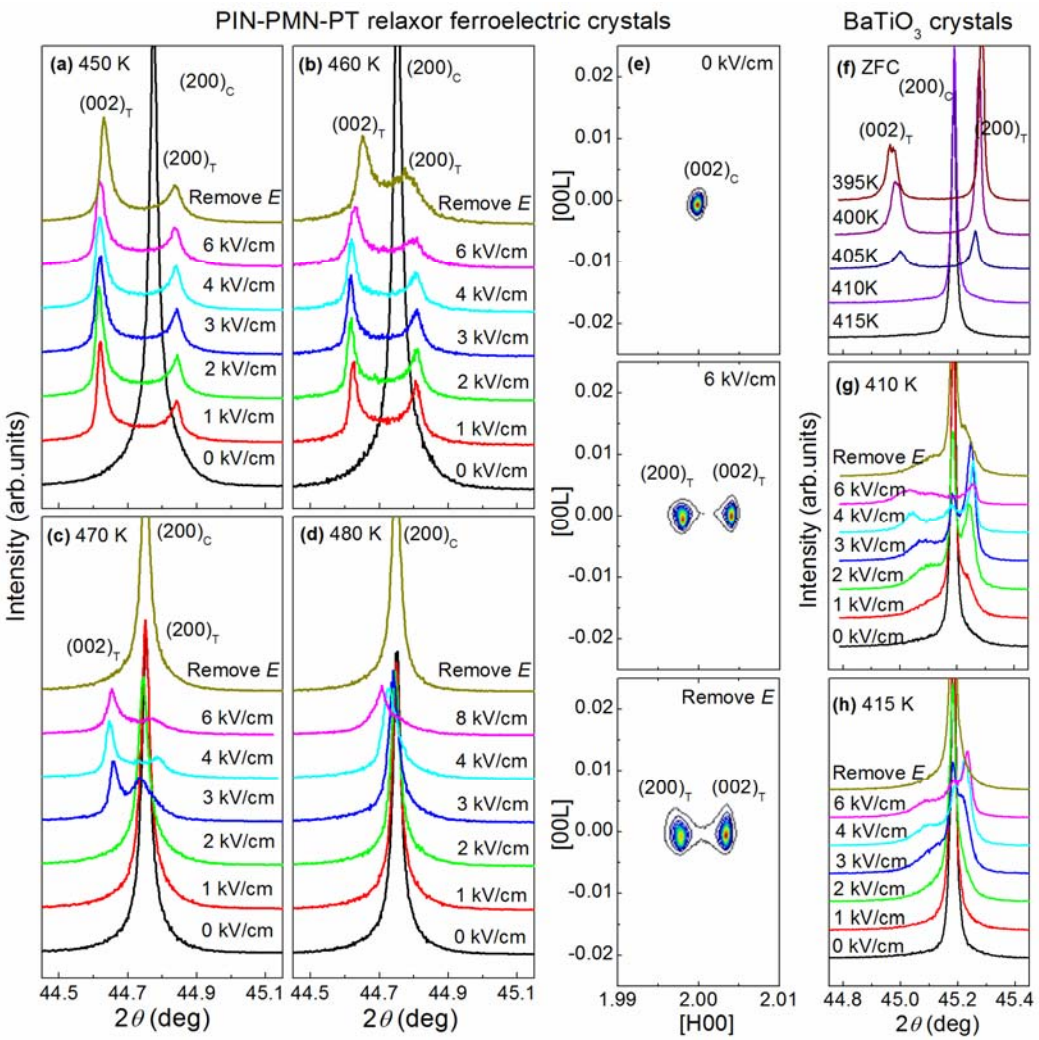

Figure 2 Diffraction data for PIN-PMN-PT relaxor ferroelectric single crystals (left three columns). Evolution of single line scans around the $(002)_{PC}$ Bragg peak with *in-situ* application of electric field along the [110] direction at (a) 450 K, (b) 460 K, (c) 470 K and (d) 480 K. (e) Reciprocal-space mesh scans at 450K under various electric field conditions. Diffraction data for $BaTiO_3$ non-relaxor ferroelectric single crystals (right column). (f) Diffraction peaks along the $(002)_{PC}$ at temperatures around Curie point under zero-field-cooling condition. Evolution of single line scans around the

$(002)_{PC}$ Bragg peak with *in-situ* application of electric field along the [110] direction at (a) 410 K and (b) 415 K.

Field-induced phase transformations were then studied above the Curie temperature (>450K). Figures 2(a-d) show the evolution of line scans through the pseudocubic (002) peak on application of electric field (*E*) parallel to the [110] direction, and after removal of *E* for four different temperatures above that of the Curie point. Several obvious features are immediately evident: (i) a tetragonal phase was induced from the cubic one under moderate field strengths below 470 K (Figures 2 a-c); (ii) the tetragonal structure persisted after removal of the field at 450 K, partially transforming back to cubic to produce coexisting *T* and *C* phase at 460 K (i.e., the *E*-field induced *T* phase was metastable at 460 K, see Figure 2b), and completely transforming back to cubic at 470 K (see Figure 2c); (iii) a tetragonal phase could not be induced under larger fields of 6kV/cm at 480 K, and the *E*-field induced *T* phase under 8kv/cm was not stable (see Figure 2d). The field-induced $C \rightarrow T$ phase transition and its persistence above Curie point was further verified by reciprocal-space mesh scans along the pseudocubic (002) peak, as shown in Fig. 2(e). A strong cubic $(002)_C$ singlet split into tetragonal $(200)_T$-$(002)_T$ twin peaks under *E* field. These twin peaks remained after removal of *E*.

It is worthy to note that such an *E*-induced metastable *T* phase in PIN-PMN-PT single crystals can be obtained over a wide temperature range (>20 K higher than Curie point), even though the persistence of an *E*-field induced ferroelectric phase

above the Curie point is a typical phenomenon for a first-order phase transition in ferroelectrics[30]. Diffraction measurements were also performed on a classic non-relaxor $BaTiO_3$ crystals along the [110] direction. Figure 2 (f) shows the evolution of line scans along the $(002)_C$ Bragg peak in the zero-field-cooling condition. The $C \rightarrow T$ phase transition occurred at 405 K, which is consistent with a dielectric anomaly[29]. The field-induced phase transformations were then studied at 410 and 415 K (Figs. 2 g and h), which are close to the Curie point. It can be seen that a doublet $(002)_T$-$(200)_T$ splitting can be induced under application of an E field parallel to the [110] direction, but a metastable T phase only existed in the C phase matrix at 410 K (i.e., weak volume fraction of T, see Figure 2g), and vanished at 415 K after removal of E. The comparison reveals that the PIN-PMN-PT relaxor ferroelectric single crystals have a notably wider temperature range of poling-induced metastable ferroelectric phase above Curie point relative to the non-relaxor $BaTiO_3$ ones.

The stability of this high temperature induced tetragonal phase in the PIN-PMN-PT single crystal (i.e., E removed at 460 K) was then studied under a zero-field-cooling condition. Figure 3(a) shows the intensity contour map of line scans along the $(002)_{PC}$ peak. Coexisting C and T phases are clearly apparent at 460 K, where the $(002)_{PC}$ peak consisted of a tetragonal (200)-(002) doublet and a cubic (002) singlet. The cubic singlet disappeared on cooling at 440 K, and the tetragonal twin peaks remained to 360 K. It is important to note that a unique diffraction behavior for the T phase was observed, relative to that typically expected from the ZFC state, on

cooling from 520 K [see Figure 1 (b)]. For the high temperature poled crystals on ZFC, the *c*-domain state was the dominate one in the tetragonal phase region. It was more pronounced on poling at temperatures slightly above the Curie point, but the *c*-domain state still retained a low volume fraction on ZFC cooling from 520 K (i.e., after annealing). Generally, the tetragonal structure has six energically equivalent polar orientations along the <001> directions in the annealed state, and two equivalent orientations (i.e., along [100] and [010]) after poling along [110]. The [110]-poled tetragonal structure exhibited a signature diffraction profile with an intensity distribution comparable to the $(200)_T$-$(002)_T$ twin peaks. However, defects or internal stress in the crystals can break such domain equivalence, resulting in some domains being weak (or even absent) compared to the equilibrium configuration[23]. In fact, recent experimental and theoretical investigations of ferroelectric materials have shown that the domain distribution can be manipulated by defect distributions[31-33]. Here, we conjecture that defect dipole pairs are oriented along the [001] direction after annealing, and thus the polar vectors of the *T* phase prefer to align along the [001]. This results in strong *a*-domain and weak *c*-domain twin peaks for diffraction measurements taken along the $(200)_{PC}$ (i.e., X-ray beam incident on the electroded faces). During poling at 460 K, defect migration may preferentially orientate the dipoles along the [100][34,35]. Such a preferential distribution has previously been reported in $BaTiO_3$ at elevated temperatures, where defect dipole pairs align along particular crystallographic axes[36]. In turn, the ferroelectric tetragonal polar vectors may be inclined to be parallel to the defect dipole, matching the symmetry[31], which

produced strong *c*-domain and weak *a*-domain peaks in the diffraction profile in the ZFC condition after poling along the [110].

On further cooling to 360 K, a phase transition was observed. The tetragonal twin peaks merged into a singlet with a high intensity. It is widely accepted that this singlet represents the rhombohedral phase. On zero field heating, this phase transition point has been called a depolarization temperature[1,37], since the piezoelectric coefficient d_{33} is significantly decreased to near zero, after having been poled at room temperature[37]. In order to further determine the structure, reciprocal-space mesh scans were performed along the $(002)_{PC}$ in the [HHL] plane after rotating the crystal by 90°. Rhombohedral and monoclinic structures can easily be distinguished by their domain configuration via this unique diffraction measurement[38,39]. The domain configuration observed here, together with the unit cells with respect to their pseudocubic one, are schematically illustrated in reciprocal-space as shown in Figs.3(b) and (c). In the (HHL) plane, there are two *c*-domains that split along the transverse direction for a monoclinic *B* (M_B) phase, where there are two *c*-domains having an angle of β-90° or 90°-β with the $[001]_{PC}$ axis[38]; whereas for the *R*-phase, there is only a singlet along this direction. Please note that monoclinic symmetry usually produces very complicated diffraction peaks[14,20], including 24 different domain configurations. However, a much simpler situation having only two domain states with distinguishable peaks prevails once the crystals are poled along unique crystallographic axes[15,20,23], as schematically illustrated in Fig.3(c).

Subsequent reciprocal-space mesh scans revealed an extremely interesting

domain configuration, as shown in Fig. 3(d). Two strong peaks split along the transverse direction were observed, which is generally designated as the finger prints of the M_B phase. Comparative diffraction measurements were also performed around the $(002)_{PC}$ Bragg peak in annealed state (i.e., cooling down to 300 K from 520 K) that was subsequently poled at room temperature along the [110], as respectively shown in Figs. 3 (e) and (f). The corresponding piezoelectric coefficient d_{33} is also given in these figures. A typical diffraction profile of the *R* phase was observed in the annealed state without piezoelectricity, and a signature domain configuration of the M_B phase was found in the [110] poled condition where d_{33} = 1600 pC/N.

The most striking finding was a M_B phase at room temperature after high temperature poling (460 K), along with a weak piezoelectric coefficient at room temperature, as shown in Fig. 3(d). These unexpected results cannot be explained by any previously reported mechanism in relaxor ferroelectric crystals[9,40,41], and are contrary to what is expected by polarization rotation theory[9]. We believe that the concept of surface effects can provide an explanation for these unconventional relationship between structure and properties. Accordingly, a surface M_B-interior *R* heterogeneous structure model is proposed, as shown in Fig. 4 (a). In this model, the surface layer of the crystal has a M_B phase with two domain states, as revealed by XRD, while the interior of the crystals has an *R* structure that is unpoled. For the annealed or unpoled *R* phase bulk of the crystal, the polar vectors are randomly oriented amongst the eight energically equivalent <111> directions, resulting in no net piezoelectricity, as shown in Fig. 4 (b). However, in the near-surface region, the M_B

phase enables the polarization to easily rotate within a plane in response to a mechanical stimuli, as illustrated Fig. 4 (c), and in turn, a large piezoelectricity may be obtained in the near surface zone.

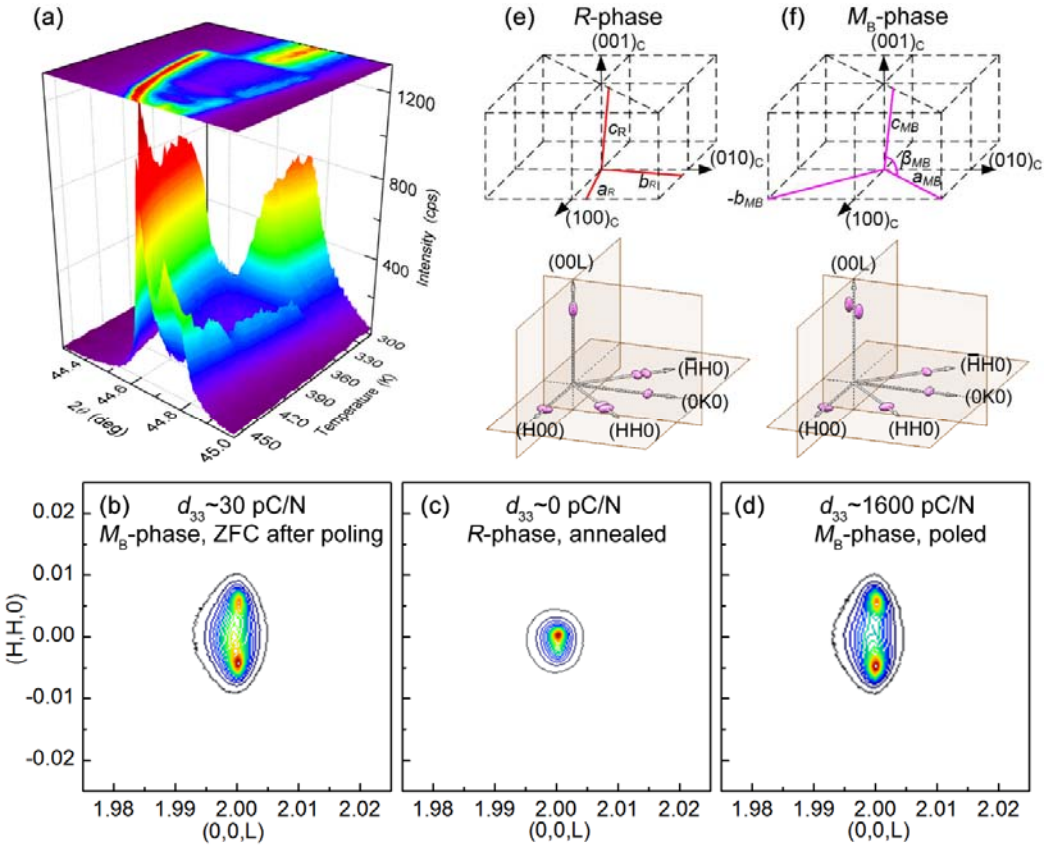

Figure 3 (a) X-ray intensity contour map consisting of line scans of the $(200)_{PC}$ Bragg peak, showing an evolution of line scans with temperature on zero-field-cooling (ZFC) after poling under a field of 6 kV/cm parallel to the [110] direction above the Curie point i.e., 460K. Reciprocal-space mesh scans around the $(002)_{PC}$ Bragg peak in the [HHL] plane for (b) ZFC after poling (i.e., poled under E = 6 kV/cm parallel to [110] at 460 K followed by ZFC to 300 K), (c) initial state (i.e., annealed at 460K for 30 min and ZFC to 300K) and (d) poled state (i.e., 300 K under E = 6 kV/cm parallel to

[110]). The corresponding piezoelectric constant d_{33} is also labeled in the respective figures. Representation of (e) rhombohedral and (f) monoclinic *B*-type unit cells with respect to the cubic one. The corresponding domain configurations in the reciprocal-space of the *R*- and M_B-phases under *E* parallel to [110] (or poled along [110]) are also illustrated in these figures[42].

Since electromechanical coupling is an integral part of both the surface and interior, surface piezoelectricity makes an important contribution to the macroscopic or average piezoelectric properties of the crystal. It is difficult to quantify precisely how much contribution was made by the surface layer. We can only speculate that the observed weak piezoelectricity can be ascribed to a thin surface layer with a high piezoelectric constant of low volume fraction. However, when the relaxor piezoelectric crystals scale-down to micro/nano-meters, the anomalous surface effect will play an increasingly important role to the average performance, as prior reports have suggested that anomalous surface effects occurs on the topmost layers (1-10 μm) of PZN-xPT, PMN-xPT, and $Na_{1/2}Bi_{1/2}TiO_3$ crystals[24,25,43,44]. In turn, the contribution of the surface layer in the "surface-interior" heterogeneous structure will be more pronounced, in particular to emerging piezoelectric MEMS/NMES devices.

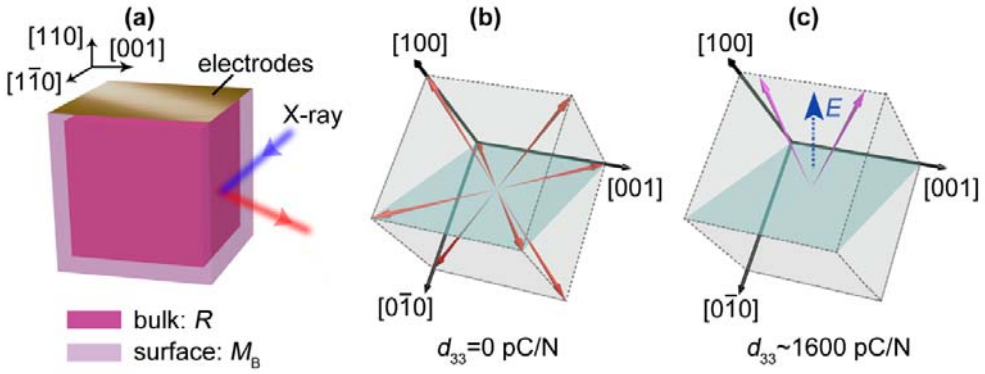

Figure 4 Schematic of (a) "surface M_B-interior R" heterogeneous structure of PIN-PMN-PT single crystals at room temperature after poling above Curie temperature. Domain configuration for (b) annealed R-phase, and (c) highly ordered M_B phase, i.e., poled or under application of field parallel to [110] direction.

Our proposed "surface-interior" heterogeneous structure is reminiscent of that reported for binary PZN-PT single crystals at high temperatures, for which a "surface ferroelectric phase-interior paraelectric phase" heterogeneous structure was shown. A labyrinthine ferroelectric domain pattern was reported in the surface layer by scanning probe techniques, whereas the bulk had an unambiguous cubic paraelectric structure above Curie point as shown by optical microscopy[24]. In these binary crystals, the surface effect was explained by compositional heterogeneity, where the surface layer was lead-deficient due to its high volatility, and B-site Nb^{5+} ions were in excess to achieve charge neutrality[24]. Besides the inconsistence of microstructure and macro-piezoelectric properties, the piezoresponse force microscopy (PFM) was also employed in order to provide more evidence to verify the proposed "surface-interior" heterogeneous structure (Figure 4), as PFM is intrinsically a surface sensitive probe

technique. Figure 5 (a) shows a schematic illustration of a "surface ferroelectric-interior paraelectric" heterogeneous structure and the working principle of the surface sensitive PFM technique. Similar to that observed in binary ferroelectric single crystals, the surface of relaxor PIN-PMN-PT single crystals exhibits a robust labyrinthine ferroelectric domain structure at temperatures several tens of degree above the Curie point, whose morphology is identical to that of ferroelectric phases (Figs. 5b-e). The domain switching hysteresis behavior and the coercive voltage at these temperature are given in Figs. 5 (f) and (g), respectively. A sharp change in the coercive voltage near the Curie point of the bulk indicate that the temperature was well-controlled during the measurements. Thus, the PFM domain structures observed above the Curie point are due to the intrinsic surface effect. The PFM results unambiguously verify that the relaxor ferroelectric materials have a depth-dependent "surface-interior" heterogeneous structure, since the cubic structure was determined by X-ray diffraction with a penetration depth of 1~2μm[23], while surface ferroelectricity was observed by PFM at temperatures several tens of degree above the Curie point.

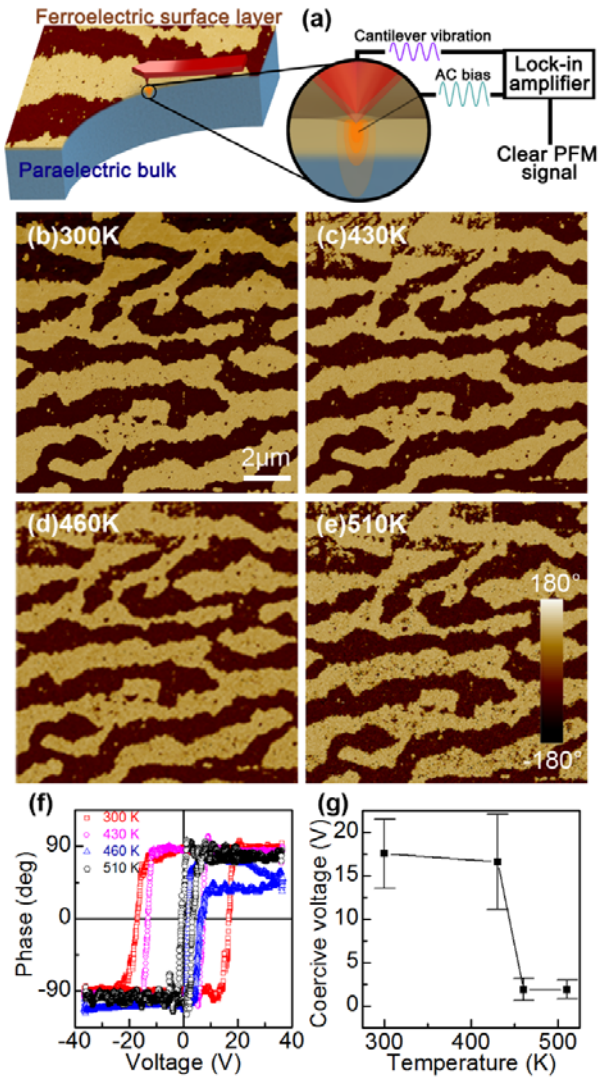

Figure 5 (a) Illustration of a "surface-interior" heterogeneous structure obtained by surface-sensitive piezoresponse force microscopy. Vertical phase image of PFM in an identical area of 10×10 μm^2 of [110]-oriented relaxor ferroelectric PIN-PMN-PT single crystal at various temperatures: (b) 300 K, (c) 430 K, (d) 460 K and (e) 510 K. (f) Tip-voltage-induced domain switching behavior at these temperatures, and (g) the corresponding temperature dependence of coercive voltage determined by the tip-voltage-induced domain switching.

Finally, the intricate phase transformation sequence in the surface layer should be discussed in more detail. The tetragonal phase of the ferroelectric relaxor single crystals belongs to the space group *P*4mm, whereas the monoclinic *B*-type phase belongs to the space group *C*m. Based on group-subgroup relationships, the $T \rightarrow M_B$ phase transformation cannot occur directly. Rather, it is only possible via an intermediate orthorhombic phase[13]. Even though only one discontinuity in the diffraction intensity and angles was observed in Fig.3 (a), it is possible to omit intermediate phases or coexistence, because our diffraction data was collected in ZFC condition at temperature intervals of 10 K. Such an intermediate phase may exist only in a narrow temperature range. For instance, it has previously been reported that an intermediate orthorhombic phase field is stable over less than a 2 K range, and that the monoclinic *C* phase field has a stability range of about 10 K which bridges M_B and *T* phases in PMN-PT crystals[45]. In fact, the reciprocal-space mesh scans in Fig. 3 (d) show indications of a coexistence of M_B and orthorhombic phases, as there is a notable continuous tail between the peaks of the doublet splitting.

IV. CONCLUSION

In summary, we have demonstrated an electric field induced metastable ferroelectric tetragonal phase above the Curie temperature on the rhombohedral side of the MPB in ternary PIN-PMN-PT relaxor single crystals by high-resolution x-ray diffraction. The *T* phase persisted above the Curie temperature, then unexpectedly transformed into a

M_B phase on zero-field cooling, exhibiting a similar domain configuration to the M_B phase induced by room temperature poling. However, the crystals with a M_B phase induced by high temperature poling had a weak piezoelectric constant of d_{33}~ 30 pC/N, which was much smaller than that of the same structure induced by poling at room temperature (i.e., d_{33}~ 1600 pC/N). A skin effect induced by a "surface M_B-interior R" heterogeneous structure was proposed to explain the inconsistency between the microstructure and macro-properties. The unique phase transition and unconventional structure-property relationship, in association with the skin effect, provide a strategy for understanding the fundamental physics of piezoelectric MEMS/NEMS devices.

ACKNOWEDGEMENTS

This work was supported by the National Natural Science Foundation of China (51602156, 51602118), the Natural Science Foundation of Jiangsu Province, China (BK20160824), the Fundamental Research Funds for the Central Universities (30916011208), and the Opening Project of Key Laboratory of Inorganic function material and device, Chinese Academy of Sciences (KLIFMD-2015-01). The X-ray diffraction data taken at Virginia Tech under the support of the Office of Naval Research (N00014-17-1-2234).

REFERENCES

[1] S. Zhang and F. Li,*High performance ferroelectric relaxor-PbTiO3 single crystals: Status and perspective.* Journal of Applied Physics **111,** 031301 (2012).

[2] E. Sun and W. Cao,*Relaxor-based ferroelectric single crystals: Growth, domain engineering, characterization and applications.* Progress in Materials Science **65,** 124 (2014).

[3] G. Y. Xu, P. M. Gehring, and G. Shirane,*Persistence and memory of polar nanoregions in a ferroelectric relaxor under an electric field.* Physical Review B **72,** 214106 (2005).

[4] Y. J. Wang, D. Gray, D. Berry, J. Q. Gao, M. H. Li, J. F. Li, and Viehland.D.,*An extremely low equivalent magnetic noise (~pT $Hz^{-1/2}$) magnetoelectric sensor.* Advanced Materials **23,** 4111 (2011).

[5] M. Zheng and R.-K. Zheng,*Electric-Field-Tunable Ferroelastic Control of Nonvolatile Resistivity and Ferromagnetic Switching in Multiferroic La0.67Ca0.33MnO3/ PbMg1/3Nb2/3O3 (0.7) PbTiO3 (0.3) Heterostructures.* Physical Review Applied **5,** 044002 (2016).

[6] S. H. Baek, J. Park, D. M. Kim, V. A. Aksyuk, R. R. Das, S. D. Bu, D. A. Felker, J. Lettieri, V. Vaithyanathan, S. S. N. Bharadwaja, N. Bassiri-Gharb, Y. B. Chen, H. P. Sun, C. M. Folkman, H. W. Jang, D. J. Kreft, S. K. Streiffer, R. Ramesh, X. Q. Pan, S. Trolier-McKinstry, D. G. Schlom, M. S. Rzchowski, R. H. Blick, and C. B. Eom,*Giant Piezoelectricity on Si for Hyperactive MEMS.* Science **334,** 958 (2011).

[7] S.-H. Baek, M. S. Rzchowski, and V. A. Aksyuk,*Giant piezoelectricity in PMN-PT thin films: Beyond PZT.* Mrs Bulletin **37,** 1022 (2012).

[8] B. Jaffe, *Piezoelectric Ceramics* (Academic Press, India, 1971).

[9] H. X. Fu and R. E. Cohen,*Polarization rotation mechanism for ultrahigh electromechanical response in single-crystal piezoelectrics.* Nature **403,** 281 (2000).

[10] D. E. Cox, B. Noheda, G. Shirane, Y. Uesu, K. Fujishiro, and Y. Yamada,*Universal phase diagram for high-piezoelectric perovskite systems.* Applied Physics Letters **79,** 400 (2001).

[11] R. Wang, H. Xu, B. Yang, Z. Luo, E. Sun, J. Zhao, L. Zheng, Y. Dong, H. Zhou, Y. Ren, C. Gao, and W. Cao,*Phase coexistence and domain configuration in $Pb(Mg_{1/3}Nb_{2/3})O_3$-0.34$PbTiO_3$ single crystal revealed by synchrotron-based X-ray diffractive three-dimensional reciprocal space mapping and piezoresponse force microscopy.* Applied Physics Letters **108,** 152905 (2016).

[12] B. Noheda, D. E. Cox, G. Shirane, J. Gao, and Z. G. Ye,*Phase diagram of the ferroelectric relaxor (1-x)$Pb(Mg_{1/3}Nb_{2/3})O_3$-x$PbTiO_3$.* Physical Review B **66,** 054104 (2002).

[13] D. Vanderbilt and M. H. Cohen,*Monoclinic and triclinic phases in higher-order Devonshire theory.* Physical Review B **63,** 094108 (2001).

[14] R. Wang, B. Yang, Z. Luo, E. Sun, Y. Sun, H. Xu, J. Zhao, L. Zheng, H. Zhou, C. Gao, and W. Cao,*Local twin domains and tip-voltage-induced domain switching of monoclinic M_C phase in $Pb(Mg_{1/3}Nb_{2/3})O_3$-0.34$PbTiO_3$ single crystal revealed by piezoresponse force microscopy.* Physical Review B **94,** 054115 (2016).

[15] Y. Wang, Z. Wang, W. Ge, C. Luo, J. Li, D. Viehland, J. Chen, and H. Luo,*Temperature-induced and electric-field-induced phase transitions in rhombohedral $Pb(In_{1/2}Nb_{1/2})O_3$-$Pb(Mg_{1/3}Nb_{2/3})O_3$-$PbTiO_3$ ternary single crystals.* Physical Review B **90,** 134107 (2014).

[16] Y. M. Jin, Y. U. Wang, A. G. Khachaturyan, J. F. Li, and D. Viehland,*Conformal miniaturization of domains with low domain-wall energy: Monoclinic ferroelectric states near the morphotropic phase boundaries.* Physical Review Letters **91** (2003).

[17] Y. U. Wang,*Three intrinsic relationships of lattice parameters between intermediate monoclinic M-C and tetragonal phases in ferroelectric Pb $(Mg_{1/3}Nb_{2/3})_{(1-x)}Ti_x$ O_3 and Pb $(Zn_{1/3}Nb_{2/3})(1-x)T_{i-x}O_3$ near morphotropic phase boundaries.* Physical Review B **73** (2006).

[18] Y. Wang, H. Ma, G. Yuan, H. Luo, and D. Viehland,*Heterogeneous domain configurations in ferroelectric crystals during thermal depolarization.* Journal of the American Ceramic Society**,** n/a (2017).

[19] D. D. Viehland and E. K. H. Salje,*Domain boundary-dominated systems: adaptive structures and functional twin boundaries.* Advances in Physics **63,** 267 (2014).

[20] B. Noheda, D. E. Cox, G. Shirane, S. E. Park, L. E. Cross, and Z. Zhong,*Polarization rotation via a monoclinic phase in the piezoelectric 92% $PbZn_{1/3}Nb_{2/3}O_3$-8% $PbTiO_3$.* Physical Review Letters **86,** 3891 (2001).

[21] G. Xu, P. M. Gehring, C. Stock, and K. Conlon,*The anomalous skin effect in single crystal relaxor ferroelectric PZN-xPT and PMN-xPT.* Phase Transitions **79,** 135 (2006).

[22] D. Phelan, E. E. Rodriguez, J. Gao, Y. Bing, Z. G. Ye, Q. Huang, J. Wen, G. Xu, C. Stock, M. Matsuura, and P. M. Gehring,*Phase diagram of the relaxor ferroelectric (1 - x)Pb($Mg_{1/3}Nb_{2/3}$)O_3-x$PbTiO_3$ revisited: a neutron powder diffraction study of the relaxor skin effect.* Phase Transitions **88,** 283 (2015).

[23] Y. Wang, D. Wang, G. Yuan, H. Ma, F. Xu, J. Li, D. Viehland, and P. M. Gehring,*Fragile morphotropic phase boundary and phase stability in the near-surface region of the relaxor ferroelectric PZN-x%PT: [001] field-cooled phase diagrams.* Physical Review B **94,** 174103 (2016).

[24] N. Domingo, N. Bagues, J. Santiso, and G. Catalan,*Persistence of ferroelectricity above the Curie temperature at the surface of Pb($Zn_{1/3}Nb_{2/3}$)O_3-12%$PbTiO_3$.* Physical Review B **91,** 094111 (2015).

[25] W. Ge, C. P. Devreugd, D. Phelan, Q. Zhang, M. Ahart, J. Li, H. Luo, L. A. Boatner, D. Viehland, and P. M. Gehring,*Lead-free and lead-based ABO(3) perovskite relaxors with mixed-valence A-site and B-site disorder: Comparative neutron scattering structural study of ($Na_{1/2}Bi_{1/2}$) TiO_3 and Pb($Mg_{1/3}Nb_{2/3}$)O_3.* Physical Review B **88,** 174115 (2013).

[26] Chrosch Jutta and E. K. H. Salje,*Near-surface Domain structures in uniaxially stressed $SrTiO_3$.* Journal of Physics: Condensed Matter **10,** 2817 (1998).

[27] F. Li, S. Zhang, Z. Xu, X. Wei, J. Luo, and T. R. Shrout,*Electromechanical properties of tetragonal Pb($In_{1/2}Nb_{1/2}$)O_3-Pb($Mg_{1/3}Nb_{2/3}$)O_3-$PbTiO_3$ ferroelectric crystals.* Journal of Applied Physics **107,** 054107 (2010).

[28] Y. Zhang, X. Li, D. Liu, Q. Zhang, W. Wang, B. Ren, D. Lin, X. Zhao, and H. Luo,*The compositional segregation, phase structure and properties of Pb($In_{1/2}Nb_{1/2}$)O_3-Pb($Mg_{1/3}Nb_{2/3}$)O_3-$PbTiO_3$ single crystal.* Journal of Crystal Growth **318,** 890 (2011).

[29] D. Fu, H. Taniguchi, M. Itoh, S.-y. Koshihara, N. Yamamoto, and S. Mori,*Relaxor Pb($Mg_{1/3}Nb_{2/3}$)O_3: A Ferroelectric with Multiple Inhomogeneities.* Physical Review Letters **103,** 207601 (2009).

[30] M.E. Lines and A. M. Glass, *Principles and applications of ferroelectrics and related materials* (Oxford University Press, Unite States, 1979).

[31] X. B. Ren,*Large electric-field-induced strain in ferroelectric crystals by point-defect-mediated reversible domain switching.* Nature Materials **3,** 91 (2004).

[32] K. Wang and J.-F. Li, *Domain Engineering of Lead-Free Li-Modified (K,Na)NbO3 Polycrystals with Highly Enhanced Piezoelectricity.* Advanced Functional Materials **20,** 1924 (2010).

[33] R.-A. Eichel, P. Erhart, P. Traeskelin, K. Albe, H. Kungl, and M. J. Hoffmann,*Defect-dipole formation in copper-doped $PbTiO_3$ ferroelectrics.* Physical Review Letters **100,** 095504 (2008).

[34] L. Luo, M. Dietze, C.-H. Solterbeck, H. Luo, and M. Es-Souni,*Tuning the functional properties of PMN-PT single crystals via doping and thermoelectrical treatments.* Journal of Applied Physics **114,** 224112 (2013).

[35] W. Ding,*Unpublication.* (2017).

[36] W. L. Warren, D. Dimos, G. E. Pike, K. Vanheusden, and R. Ramesh,*ALIGNMENT OF DEFECT DIPOLES IN POLYCRYSTALLINE FERROELECTRICS.* Applied Physics Letters **67,** 1689 (1995).

[37] Y. Wang, H. Ma, G. Yuan, H. Luo, and D. Viehland, *Heterogeneous domain configurations in ferroelectric crystals during thermal depolarization.* Journal of the American Ceramic Society **100,** 1751 (2017).

[38] J. Yao, H. Cao, W. Ge, J. Li, and D. Viehland,*Monoclinic M-B phase and phase instability in 110 field cooled $Pb(Mg_{1/3}Nb_{2/3})O_3$-30%$PbTiO_3$ single crystals.* Applied Physics Letters **95,** 052905 (2009).

[39] H. Cao, F. M. Bai, N. G. Wang, J. F. Li, D. Viehland, G. Y. Xu, and G. Shirane,*Intermediate ferroelectric orthorhombic and monoclinic M_B phases in 110 electric-field-cooled $Pb(Mg_{1/3}Nb_{2/3})O_3$-30%$PbTiO_3$ crystals.* Physical Review B **72,** 064104 (2005).

[40] D. Phelan, C. Stock, J. A. Rodriguez-Rivera, S. Chi, J. Leao, X. Long, Y. Xie, A. A. Bokov, Z.-G. Ye, P. Ganesh, and P. M. Gehring,*Role of random electric fields*

in relaxors. Proceedings of the National Academy of Sciences of the United States of America **111,** 1754 (2014).

[41] F. Li, S. Zhang, T. Yang, Z. Xu, N. Zhang, G. Liu, J. Wang, J. Wang, Z. Cheng, Z.-G. Ye, J. Luo, T. R. Shrout, and L.-Q. Chen,*The origin of ultrahigh piezoelectricity in relaxor-ferroelectric solid solution crystals*. Nature Communications **7,** 13807 (2016).

[42] H. Cao, Thesis, Virginia Tech, 2008.

[43] G. Y. Xu, H. Hiraka, G. Shirane, and K. Ohwada,*Dual structures in (1-x)Pb($Zn_{1/3}Nb_{2/3}$)O_3-x$PbTiO_3$ ferroelectric relaxors.* Applied Physics Letters **84,** 3975 (2004).

[44] G. Y. Xu, D. Viehland, J. F. Li, P. M. Gehring, and G. Shirane,*Evidence of decoupled lattice distortion and ferroelectric polarization in the relaxor system PMN-xPT.* Physical Review B **68,** 212410 (2003).

[45] Z. Kutnjak, R. Blinc, and Y. Ishibashi,*Electric field induced critical points and polarization rotations in relaxor ferroelectrics.* Physical Review B **76,** 104102 (2007).

Figure Captions

Figure 1 (a) Dielectric constant dependence on temperature under zero-field-cooling condition. (b) Intensity contour map of $(002)_{PC}$ Bragg peaks that show the evolution of phase transformation with temperature under a zero-field-cooling condition. (c) Full width of half maximum (FWHM) of the $(002)_{PC}$ Bragg peak of non-relaxor ferroelectric $BaTiO_3$ and relaxor ferroelectric PIN-PMN-PT single crystals in the

cubic phase region. (d) Diffraction peaks along the $(002)_{PC}$ at various temperatures for PIN-PMN-PT crystals under zero-field-cooling condition.

Figure 2 Diffraction data for PIN-PMN-PT relaxor ferroelectric single crystals (left three columns). Evolution of single line scans around the $(002)_{PC}$ Bragg peak with *in-situ* application of electric field along the [110] direction at (a) 450 K, (b) 460 K, (c) 470 K and (d) 480 K. (e) Reciprocal-space mesh scans at 450K under various electric field conditions. Diffraction data for $BaTiO_3$ non-relaxor ferroelectric single crystals (right column). (f) Diffraction peaks along the $(002)_{PC}$ at temperatures around Curie point under zero-field-cooling condition. Evolution of single line scans around the $(002)_{PC}$ Bragg peak with *in-situ* application of electric field along the [110] direction at (a) 410 K and (b) 415 K.

Figure 3 (a) X-ray intensity contour map consisting of line scans of the $(200)_{PC}$ Bragg peak, showing an evolution of line scans with temperature on zero-field-cooling (ZFC) after poling under a field of 6 kV/cm parallel to the [110] direction above the Curie point i.e., 460K. Reciprocal-space mesh scans around the $(002)_{PC}$ Bragg peak in the [HHL] plane for (b) ZFC after poling (i.e., poled under E = 6 kV/cm parallel to [110] at 460 K followed by ZFC to 300 K), (c) initial state (i.e., annealed at 460K for 30 min and ZFC to 300K) and (d) poled state (i.e., 300 K under E = 6 kV/cm parallel to [110]). The corresponding piezoelectric constant d_{33} is also labeled in the respective figures. Representation of (e) rhombohedral and (f) monoclinic *B*-type unit cells with respect to the cubic one. The corresponding domain configurations in the

reciprocal-space of the *R*- and M_B-phases under *E* parallel to [110] (or poled along [110]) are also illustrated in these figures[42].

Figure 4 Schematic of (a) "surface M_B-interior *R*" heterogeneous structure of PIN-PMN-PT single crystals at room temperature after poling above Curie temperature. Domain configuration for (b) annealed *R*-phase, and (c) highly ordered M_B phase, i.e., poled or under application of field parallel to [110] direction.

Figure 5 (a) Illustration of a "surface-interior" heterogeneous structure obtained by surface-sensitive piezoresponse force microscopy. Vertical phase image of PFM in an identical area of 10×10 μm^2 of [110]-oriented relaxor ferroelectric PIN-PMN-PT single crystal at various temperatures: (b) 300 K, (c) 430 K, (d) 460 K and (e) 510 K. (f) Tip-voltage-induced domain switching behavior at these temperatures, and (g) the corresponding temperature dependence of coercive voltage determined by the tip-voltage-induced domain switching.